Am J Nucl Med Mol Imaging 2018;8(6):387-396
www.ajnmmi.us /ISSN:2160-8407/ajnmmi0087094

Original Article

Metabolic and densitometric correlation between atherosclerotic plaque and trabecular bone: an ^{18}F-Natrium-Fluoride PET/CT study

Francesco Fiz[1,2], Matteo Bauckneht[3], Arnoldo Piccardo[4], Cristina Campi[5], Alberto Nieri[3], Roberta Piva[3], Giulia Ferrarazzo[3], Nathan Artom[6], Silvia Morbelli[3], Cecilia Marini[7], Michele Piana[8,9], Marcello Bagnasco[1], Marco Canepa[10], Gianmario Sambuceti[3]

[1]Department of Internal Medicine, University of Genoa, Italy; [2]Nuclear Medicine Unit, Department of Radiology, University of Tübingen, Germany; [3]Nuclear Medicine Unit, Department of Health Sciences, University of Genoa, Italy; [4]Nuclear Medicine Unit, Galliera Hospital, Genoa, Italy; [5]Nuclear Medicine Unit, Department of Medicine-DIMED, University Hospital of Padua, Italy; [6]Department of Internal Medicine, Local Healthcare Unit, Savona, Italy; [7]CNR-IBFM, Genoa, Italy; [8]CNR-SPIN, Genoa, Italy; [9]Department of Mathematics, University of Genoa, Italy; [10]Department of Cardiology, University of Genoa, Italy

Received August 1, 2018; Accepted October 24, 2018; Epub December 20, 2018; Published December 30, 2018

Abstract: Increasing evidence links atherosclerosis to a decreased bone thickness. This correlation could reflect a bone/plaque interaction. Hereby we analyzed Hounsfield density (HU) and mineral turnover in bone and in the arterial calcifications (AC), using a computational method applied to PET/CT data. 79 ^{18}F-NaF PET/CT from patients with AC were retrospectively analyzed. Mean AC density and background-corrected uptake (TBR) were estimated after semi-automatic isocontour segmentation. The same values were assessed in the trabecular bone, using an automatic adaptive thresholding method. Patients were then stratified into terciles, according to their mean HU plaque density ("light", "medium" or "heavy" calcifications"). 35 ^{18}F-NaF PET/CT from patients without AC served as controls. Vertebral density and TBR were lower in patients than in controls (137±25 vs. 160±14 HU, P<0.001); (6.2±3.9 vs. 8.4±3.4, P<0.05). Mean trabecular TBR values were 8.3±4, 4.5±2.1 and 3.5±1.8 in light, medium and heavy AC groups, respectively (P<0.05 for light vs. medium and P<0.01 for light vs. heavy). Similarly, mean trabecular HU was 143±19, 127±26 and 119±18 in the three groups, respectively (P<0.01 for light vs. heavy). Mean AC density was inversely associated with the trabecular HU (R=-0.56, P<0.01). Conversely, plaques' TBR directly correlated with the one in trabecular bone (R=0.63, P<0.001). At multivariate analysis, the sole predictor of vertebral density was plaque HU (P<0.05). Our data highlight a correlation between plaque and bone morpho-functional parameters and suggest that observing skeletal bone characteristics could represent a novel window on atherosclerosis pathophysiology.

Keywords: Positron emission tomography, atherosclerosis, bone density, computational analysis

Introduction

Cardiovascular disease is a widespread health problem, causing more mortality and morbidity than any other disease, not only in advanced economies but also in emerging middle-low income countries [1]. The hallmark of this ailment is atherosclerosis; there is now overwhelming evidence that these lesions do begin at a very early age and that the plaque build-up process spans over decades [2-5]. Evolution of atherosclerotic plaques can, however, occur at a variable rate, according to presence, degree, and duration of risk factors. Radiological evidence of calcification is a relatively late hallmark of vascular lesions, representing an advanced stage of disease progression as well as a marker of increased morbidity risk [6]. However, there are accumulating data suggesting that processes leading to calcification could begin early in the plaque's natural history [7, 8]; moreover, patients with elevated cardiovascular risk profile appear having a higher mineral turnover within the vascular wall of large and small vessels [9-11].

This evidence fosters the concept of the atherosclerotic disease as a systemic, rather than a

local, ailment, in which whole-body modifications promote a "plaque-promoting" environment [12-17]. Calcification represents the late stages of plaque evolution, in which the atherosclerotic lesion becomes apparent at x-ray-based imaging. Remarkably, the same molecular mediators of arterial calcifications, such as those belonging to the RANKL-RANK-Osteoprotegerin axis [15, 16], are also involved in bone turnover and can influence bone density: acting on RANKL with a specific inhibitor has proved effective in halting and even reversing osteoporosis [18].

Accordingly, it has been proposed that plaque build-up and osteoporotic degeneration might be mediated by common factors [19, 20]. This hypothesis is supported by the evidence that the degree of arterial calcification is linked to progressive loss of bone density as well as to increased fracture risk [21, 22]. It could be hypothesized that, in the scenario of diffuse atherosclerotic disease, the presence of inflammation may release specific mediators, which could stimulate an acceleration in mineral turnover even in areas remote to the plaques [15, 23]. Such a mechanism could explain the increased plaque calcium deposition and the impoverishment of the bone mineral density that is observed in these subjects.

In this sense, the status of bone density could represent a window on the processes of an ongoing arterial calcification process; moreover, interventions aimed at restoring bone density could also take effect on the plaque's build-up.

Testing this hypothesis requires a method able to detect both calcium density and mineral metabolism at the same time. The technological development of hybrid imaging, comprising multi-detector CT and 3D-positron-emission tomography (PET/CT) might allow for such evaluations [24]. An ever-increasing number of reports have described the exploitation of ^{18}F-Natrium-Fluoride (^{18}F-NaF) to detect calcium deposition within the actively growing plaque [25-28]. Our previous experience showed that this approach has a more significant validity in the earlier stages of plaque formation, while the calcification pathways are most active [7, 15]. In the present study, ^{18}F-NaF-PET/CT images were analyzed with a two-way approach: measurement of mineral metabolism and calcification density within plaques, as well as in trabecular bone. In doing so, we tested the hypothesis that increased plaque density is linked with loss of bone mineral content and that the activation of mineral metabolism within the atherosclerotic plaque is paralleled by a similar activation in the trabecular bone.

Materials and methods

Patient populations

The study included 79 patients with either breast (65%) or prostate (35%) cancer undergoing ^{18}F-NaF PET/CT scan for suspected bone metastases or for monitoring of known ones.

Patients were included in the analysis if they presented at least one CT-evident arterial calcification (AC) in the infrarenal abdominal aorta. AC was defined as a mural area of calcium deposition, with a minimum HU of 130 and evident in at least five consecutive CT slices [26]. This size requirement was chosen to avoid a partial-volume effect in the evaluation of PET uptake.

Exclusion criteria were: history of vasculitis, autoimmune or systemic inflammatory disease as well as chemo- or radiotherapy in the preceding 8 weeks, as previously proposed [9]. Chronic steroid therapy represented an additional exclusion factor. Cardiovascular risk profile was assessed in each patient (including age, sex, diabetes, smoking, hypertension, dyslipidemia and body mass index).

35 age- and sex-matched patients, having no evidence of arterial calcifications were randomly selected from our pool of ^{18}F-NaF-PET/CT examinations and used as plaque-free controls.

Written informed consent was obtained from each patient before the exam, including the permission to use pseudonomyzed imaging data for research purpose. Institutional Ethics Committee approved this retrospective study and the requirement to obtain additional informed consent for this specific analysis was waived.

^{18}F-NaF PET/CT acquisition and images reconstruction

Patients underwent ^{18}F-NaF PET/CT using two 16 slices PET/CT hybrid systems: (1) Biograph

Table 1. Clinical characteristics of the patients' population

Clinical variables	All Patients with Plaques N=79	No metastases N=19	Evidence of Metastases N=60	Controls N=35	*P* value (Metastases vs. no Metastases)	*P* value (Patients vs. Controls)
Age, years	70.8±8.04	70.5±10.5	70.9±7.17	72.4±6.1	NS	NS
Women	65%	89%	57%	45%	0.009	NS
Previous chemotherapy	41%	11%	51%	62%	0.002	0.045
Previous radiotherapy	55%	32%	63%	65%	0.02	NS
Previous chemo- or radiotherapy	63%	32%	73%	81%	0.001	0.039
Previous chemo- and radiotherapy	29%	11%	35%	43%	0.04	NS
Body mass index, kg/m^2	25.3±4.6	26.9±3.6	24.8±4.8	23.2±2.8	NS	NS
Obese (body mass index ≥30 kg/m^2)	9%	16%	7%	6%	NS	NS
Smoking history	58%	57%	58%	N/A	NS	-
Hypertension	67%	69%	65%	N/A	NS	-
Antihypertensive medications	66%	77%	61%	N/A	NS	-
Dyslipidemia	46%	43%	47%	N/A	NS	-
Lipid-lowering medications	25%	31%	24%	N/A	NS	-
Diabetes	29%	50%	21%	N/A	0.03	-
Bisphosphonates	7%	0%	7%	N/A	NS	-
Warfarin	7%	0%	7%	N/A	NS	-
Proton pump inhibitors	31%	29%	31%	N/A	NS	-

WB: Whole-body.

16 (Siemens Medical Solutions, Knoxville TN, United States); and (2) Discovery LS (GE Medical Systems, Milwaukee, WI, United States). In both cases patients received an intravenous bolus injection of ^{18}F-NaF (4.8-5.2 MBq per kilogram of body weight). PET/CT acquisition started 60-75 min thereafter, in the meantime the patient was hydrated and encouraged to void, as to diminish the unbound tracer fraction. The entire body was scanned from vertex to toes in an "arms down" position; emission scan lasted 120 seconds per bed position. PET raw data were reconstructed by means of ordered subset expectation maximization (OSEM, 3 iterations, 16 subsets) and attenuation correction was performed using CT data. The transaxial field of view and pixel size of the reconstructed PET images were 58.5 cm and 4.57 mm, respectively, with a matrix size of 128 × 128 mm. As per standard PET/CT imaging protocol, 16-detector row helical CT scan was performed with non-diagnostic current and voltage settings (120 Kv, 80 mA), with a gantry rotation speed of 0.5 s and table speed of 24 mm per gantry rotation. No contrast medium was injected. The entire CT dataset was fused with the 3-dimensional PET images using an integrated software interface (Syngo; Siemens Erlangen, Germany). Low dose CT (reconstructed at 4 mm thick slices) was used for anatomical reference for the localization of vascular calcification.

Plaque analysis

Image analysis was carried out with 64-bit Osirix DICOM viewer (Pixmeo, Geneva, CH) and with PMOD software package (v. 3.4, PMOD Technologies, Zurich, CH). ACs were excluded from the analysis if there was considerable suspect of spill-over from a nearby structure (e.g. lumbar vertebrae). In case of doubt, a safety margin of 1-cm from the bone edge was used.

For both CT and PET aortic measurements the whole aorta was considered, including the ascending, descending and infrarenal segments. CT images were used to semi-automatically draw volumes of interest (VOI) on each AC site, using a region-growing algorithm, whose lower limit was set at 130 HU. In each VOI, average HU was calculated. In addition, an Agatston-like calcium score (CS) was calculated with a dedicated software application (Osirix DICOM viewer, Pixmeo, Geneva, CH). Thereafter, average SUV was computed in each VOI using the co-registered PET data. These values were normalized for blood-pool radioactivity, which was

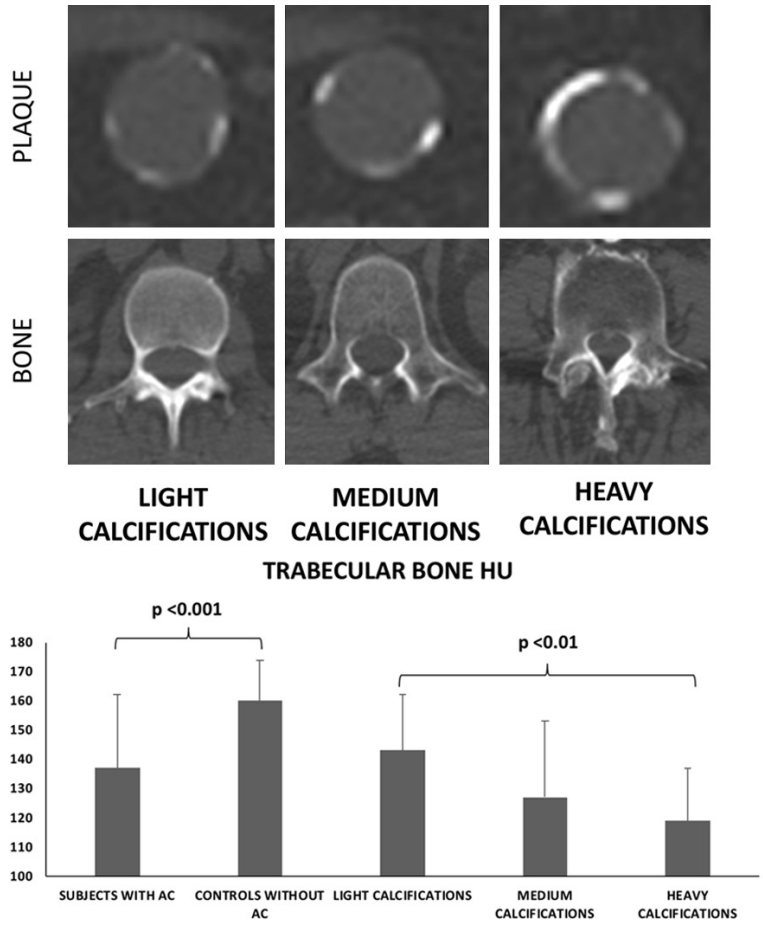

Figure 1. Density trabecular bone and in the aortic plaque. In the three top panels are displayed low-dose CT images depicting examples of typical "light", "medium" and "heavy" plaques. Directly below (middle panels) are displayed CT slices of the trabecular bone from the same patients. After terciles stratification according to mean plaque density, subjects with a higher mean plaque thickness presented a decreased vertebral density and metabolism (lower histogram).

obtained by drawing a 10-slice thick VOI on the inferior vena cava, to obtain plaque target-to-background ratio (TBR).

Computational analysis of trabecular bone

Bone image analysis was performed semi-automatically according to a previously validated method [29-32]. Briefly, the algorithm identifies the skeleton on CT images assuming that compact bone is the structure with the highest radiograph attenuation coefficient in the human body. Once it has identified the skeletal border, the program starts the thresholding algorithm, which samples a 2-voxel-thick layer and computes its average Hounsfield Unit (HU) value. Thereafter, all skeletal voxels having attenuation coefficient equal or above this value are considered as compact bone, and the remaining as trabecular bone. This latter volume is then voxel-wise multiplied against the PET co-registered data to extract and represent bone marrow metabolic activity. For the purpose of the present analysis, thoracic and lumbar vertebrae were selected as representative bone regions.

This above-described segmentation method can tell apart osteoblastic metastases from normal trabecular bone [33]. Moreover, the software removes all voxels under a 100 HU threshold, effectively excluding lytic metastases. Therefore, it is possible to analyze trabecular bone metabolism without the influence of uptake from tumor localizations. However, effects due to radioactivity spill-over from nearby lesion or presence of mixed-type metastases within trabecular bone cannot be denied with utmost security by the automated analysis. For this reason, two expert readers (SM and GMS) reviewed the output images and manually removed all bone regions with suspicious metastatic involvement.

Statistical analysis

All data are reported as Mean ± SD. Patients with ACs were stratified in three groups according to their tercile of mean plaque density: patient with a mean calcification in the lower tercile were defined as with "light" calcifications, while those in the middle and upper terciles were defined as having "medium" and "heavy" calcifications, respectively. Differences between groups were tested using one-way analysis of variance, with intergroup comparison afforded using Bonferroni test. Correlation was tested used bivariate analysis (Pearson's R

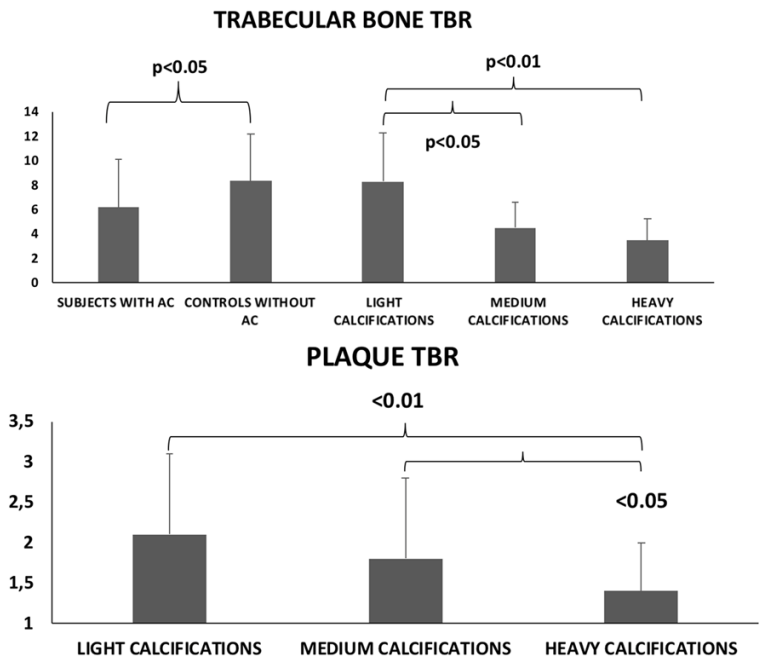

Figure 2. Mineral metabolic activity in patients and controls. The histograms depict the target-to-background ratio of subjects with a ACs and of controls in trabecular bone (upper) and the corresponding value within the plaques. Subjects with ACs had a lower TBR than controls; however, this metabolic decrease was circumscribed to patients with medium and heavy calcifications. Likewise, plaque TBR was higher in less heavily calcified plaques.

as well as by multiple linear regression analysis. *p* values <0.05 were considered as statistically significant. Statistical analyses were performed using SPSS software Advanced Models 24 (IBM, Chicago, Illinois, US).

Results

Characteristics of the study population

Out of the 79 study patients, 60 (76%) had evidence of bone localizations while 19 (24%) had no highlightable metastases. **Table 1** lists the main characteristics of the study population, including a comparison of patients with and without bone metastases. The prevalence of major cardiovascular risk factors and medications did not differ between these groups, except for a slightly higher prevalence of diabetes in those without bone metastases (50% vs. 21% in those with metastases, P=0.03). The only significant difference in ^{18}F-NaF PET/CT-derived parameters was a higher aortic mean HU in those patients with evidence of bone metastases (241.8±58.7 vs. 241.8±58.7 in those without metastases, P=0.03). There were no other differences in bone-related parameters.

On the basis of the tercile stratification, the "heavy" and "medium" calcifications' groups counted 26 patients each and the remaining 27 patients were placed in the "light" calcification group.

Uptake and calcification indices

In patients with ACs, mean TBR in the trabecular bone was 6.2±3.9 and mean trabecular bone density was 137±25 HU. The mean TBR of all aortic plaques was 1.9±1.2, with a mean HU density of 227±61. Control patients without ACs had a markedly higher vertebral density (160±14 HU, P<0.001 vs. patients with plaques) and a slightly higher mineral metabolism (TBR 8.4±3.4, P<0.05 vs. patients with plaques). Among the patients with ACs, a progressive reduction in mineral metabolism as well as in trabecular bone density can be observed when comparing the three subgroups, whereas patients with "heavy" calcifications show significantly reduced values in comparison with these with "light" arterial calcium deposits.

In fact, mean trabecular TBR values were 8.3±4, 4.5±2.1 and 3.5±1.8 in light, medium and heavy calcifications' groups, respectively (P<0.05 for light vs. medium and P<0.01 for light vs. heavy). Similarly, mean trabecular HU was 143±19, 127±26 and 119±18 in the three groups, respectively (P<0.01 for light vs. heavy). Finally, uptake intensity within the plaque dwindled when progressing from heavy to light calcifications (TBR: 2.1±1; 1.8±1 and 1.4±0.6 for light, medium and heavy calcifications, respectively, P<0.05 for medium vs. heavy and P<0.01 for light vs. heavy). See **Figures 1**, **2** and **Table 2** for details.

Interaction between plaque and bone

Mean plaque density showed an inverse association with vertebral HU density (R=-0.56, P<0.01, **Figure 3**). In opposition, no correlation

Table 2. Radiological characteristics of the patients' population

^{18}F-NaF PET/CT variables	All Cases with plaques N=79	Group I: no metastases N=19	Group II: metastases N=60	Controls without plaques N=35	*P* value (group I vs. group II)	*P* Value (plaques vs. controls)
Bone variables						
Bone mean HU	137±25	135±31	126±18	160.3±14	NS	<0.001
Bone mean TBR	6.2±3.9	5.9±2	6.4±4.5	8.4±3.8	NS	0.034
Aortic plaque variables						
Aortic mean HU	227±71	206±65	245±59	-	0.026	-
Aortic mean TBR	1.9±1.2	1.9±1.4	2±1.1	-	NS	-
Infrarenal aortic diameter, mm	18.6±4.4	18.1±1.6	18.8±4.9	-	NS	-

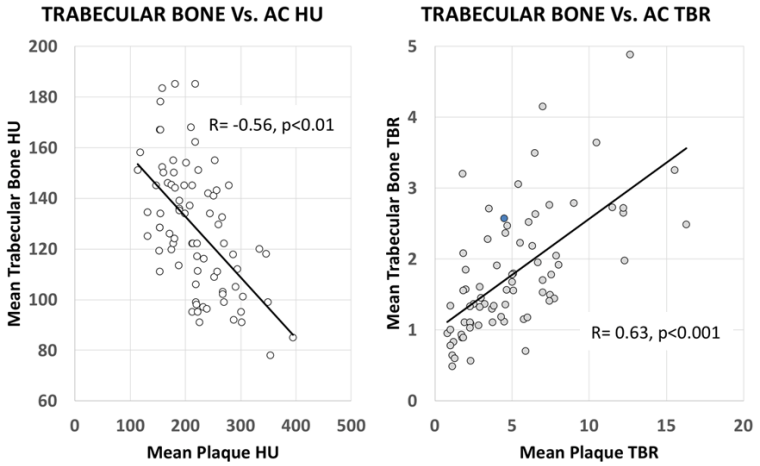

Figure 3. Correlation between vertebral density and plaque features. A higher plaque density was associated to a lower trabecular density; conversely, TBR in the AC was directly associated with the one in the trabecular skeleton.

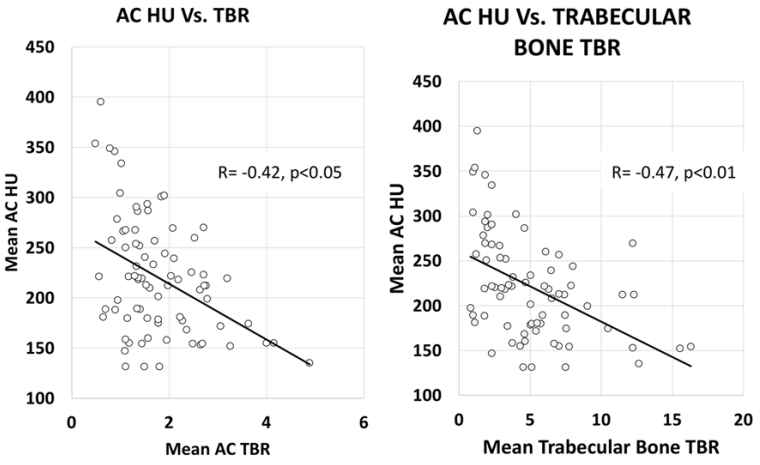

Figure 4. Correlation between plaque and trabecular mineral metabolism. Patients with thicker arterial calcifications showed a reduced mineral metabolism within the plaque itself and in the trabecular bone.

between age and HU density was observed.

Conversely, plaque and trabecular bone TBR were directly and closely correlated (R=0.63 and P<0.001, **Figure 3**).

Arterial plaque HU density displayed an inverse correlation with its own TBR (R=-0.42, P<0.05, **Figure 4**), as well as with lumbar vertebrae TBR (R=-0.47, P<0.01, **Figure 4**).

Multiple regression analysis of plaque density and metabolism

At univariate analysis, mean HU density of aortic plaque was not predicted by any of the cardiovascular risk factor or by age; conversely, it was related to its own TBR (P≤ 0.001) as well as by trabecular bone TBR (see **Table 3** for details). Mean vertebral density was related only to plaque density (P<0.05); conversely age, use of bisphosphonates and previous radio/chemotherapy had no influence on vertebral status (**Table 4**).

Discussion

Our results show the existence of a correlation between mineral metabolism in the arterial plaque and in the trabecular skeleton. This connection can be highlighted both on the morphologic as well as on the metabolic plane. From the

Table 3. Multiple regression analysis of parameter influencing aortic plaque density (HU)

Variable	Standardized Coefficient		Sig.	95% Confidence Interval	
	Beta	t		Lower Bound	Upper Bound
Age	0.168	1.503	NS	-0.407	2.91
Gender	-0.033	-0.296	NS	-32.12	23.813
Smoking History	-0.108	-0.929	NS	-29.935	10.896
Hypertension	0.032	0.271	NS	-23.938	31.486
Diabetes	0.025	0.21	NS	-28.048	34.648
Dyslipidaemia	0.061	0.51	NS	-20.355	34.339
Aortic Plaques TBR	-0.401	-3.786	<0.001	-43.009	-13.351
Mean trabecular TBR	-0.558	-3.863	<0.001	-14.966	-4.641

Table 4. Multiple regression analysis of parameter influencing vertebral density (HU)

Variable	Beta	t	Sig.	95% Confidence Interval for B	
				Lower Bound	Upper Bound
Chemotherapy	-.154	-.685	NS	-31.308	16.077
Radiotherapy	.370	1.658	NS	-4.738	37.925
Bisphosphonates	-.215	-1.188	NS	-68.115	19.372
BMI	.342	1.643	NS	-.711	5.489
Age	-.045	-.220	NS	-1.419	1.154
Gender	.247	1.15	NS	-0.856	1.152
AC Density (HU)	-.546	-2.671	.014	-.398	-.051
Mean trabecular TBR	-.050	-.214	NS	-3.347	2.737
Mean AC TBR	-.105	-.331	NS	-22.264	16.278

morphological point of view, it was already established that patients with arterial calcifications suffer from reduced calcium density and are at increased risk for bone fractures [21, 34, 35]. In particular, Kiel et al. analyzed patients from the Framingham study cohort longitudinally and suggested that the association between arterial calcification and the bone mineral content reduction could be more than a simple age-related random association. Actually, in our study, patients with and without aortic calcifications had no significant age differences; however, the ones with calcifications had markedly reduced bone density. Moreover, patients with extended and thick arterial calcifications had a greater bone density impairment when compared to those with early-stage arterial lesions.

From the metabolic point of view, the presence of calcification was related to reduce metabolic activity within the trabecular bone. Similar to bone density, the impairment was greatest in the group with the thickest calcifications. Since the uptake of sodium fluoride in the osseous matrix reflects the rate of new bone formation [36-38], it may follow that a reduced uptake is caused by a reduced bone-deposition activity or by an augmented bone erosion. In our series, the multivariate analysis showed that external therapy (including bisphosphonates), age and BMI were not associated with the trabecular thickness; the only relevant predictor of bone density was the arterial calcification thickness. It might be hypothesized that factors produced within the plaque microenvironment and relevant for the plaque progression, including RANKL, which is also a potent osteoclast activator [15, 39], could be able to act on the remote skeletal tissue. On the other hand, if bone resorption and calcium deposition are governed by similar mechanisms, then contrasting bone resorption could have beneficial effects on arterial calcifications as well. This hypothesis has been to this date scarcely investigated: the only available data come from a subpopulation of the FREEDOM study, where the effect of a long-lasting Denosumab (a specific RANKL antibody) therapy on cardiovascular risk and calcification progression were tested against a placebo. The study failed to demonstrate a cardiovascular benefit of the drug over a three-year period (a non-significant 2% reduction of cardiovascular risk was observed). However, this study included the female gender only, with 91% of patients being older than 70 years. Moreover, the follow-up period was limited to three years. Therefore, it is unknown whether this approach would be

effective if applied to the male gender, if started at an earlier age or if its effects are evaluated on a more extended time-span. In fact, considering the long-term course of the atherosclerotic disease, a continuous therapy might be in order to achieve full effect. Even if the anti-resorption therapy should prove unsuccessful in delimiting plaque growth, it could nonetheless be used to prevent bone loss and consequently to limit the fracture risk in these patients [40].

Finally, there was an inverse correlation between plaque density and its mineral metabolism. This phenomenon has been already investigated in our previous study [7] and it's likely to reflect the different stages of active and passive calcifications within plaques [26].

Overall, our study demonstrates a decreasing trend in bone density as well as in bone and plaque mineral metabolism, as the arterial plaques grow and become thicker. This pattern is progressive and a difference between subjects with and without arterial calcifications can be observed in the earlier stages of vascular calcium deposition. As the disease progresses and the plaque accumulates more calcium, changes within the remote bone tissue become steadily more pronounced. These data suggest that observation of bone morphologic and metabolic patterns could represent a window in the evaluation of the pathophysiology of the atherosclerotic plaque. Further studies are needed to determine the exact molecular mechanism and to test a possible way to influence the plaque progression by acting on mineral metabolism.

The present study is affected by some limitations. It is a dual-center retrospective study, enrolling the only possible population for analysis of ^{18}F-NaF distribution, i.e. prostate and breast cancer patients, submitted to the exam for known or suspected metastases. While this has no influence on plaque uptake, the presence of skeletal localizations could have impacted the uptake on neighboring voxels, both due to the different resolution of PET and CT as well as for the static effect of skeletal metastases on healthy tissue metabolism [41, 42]. For these reasons, a manual correction was used in all cases to eliminate any spillover artifact after the automatic bone segmentation. A further limitation is that, although we demonstrated a decreased trabecular density in patients with thicker plaques, we had neither DEXA scan data nor mineral metabolism blood values at disposal. Further prospective studies, enrolling patients with planned ^{18}F-NaF PET/CT controls and known cardiovascular disease, could shed light on these aspects.

Conclusion

The present study suggests the occurrence of a systemic interplay between trabecular bone and the atherosclerotic plaque. While the determinants of such correlation remain yet to be identified, our data highlight a progressive impairment of the bone structure with progressing aortal atherosclerosis. In this context, the bone might serve as a window on the disease status in patients with atherosclerosis. Further research could verify, also with preclinical studies, the potential efficacy of bone-active drugs on the progression of the arterial plaque and thus possibly foster novel anti-plaque strategies.

Acknowledgements

Informed consent was obtained from all individual participants included in the study.

Disclosure of conflict of interest

None.

Address correspondence to: Francesco Fiz, Nuclear Medicine Unit, Department of Radiology, University of Tübingen, Otfried-Müller Straße 14, Tübingen 72076, Germany. E-mail: francesco.fiz.nm@gmail.com

References

[1] Liu Y, Dalal K and Stollenwerk B. The association between health system development and the burden of cardiovascular disease: an analysis of WHO country profiles. PLoS One 2013; 8: e61718.

[2] Tuzcu EM, Kapadia SR, Tutar E, Ziada KM, Hobbs RE, McCarthy PM, Young JB and Nissen SE. High prevalence of coronary atherosclerosis in asymptomatic teenagers and young adults: evidence from intravascular ultrasound. Circulation 2001; 103: 2705-2710.

[3] Hong YM. Atherosclerotic cardiovascular disease beginning in childhood. Korean Circ J 2010; 40: 1-9.

[4] Joseph A, Ackerman D, Talley JD, Johnstone J and Kupersmith J. Manifestations of coronary atherosclerosis in young trauma victims--an autopsy study. J Am Coll Cardiol 1993; 22: 459-467.
[5] Virmani R, Robinowitz M, Geer JC, Breslin PP, Beyer JC and McAllister HA. Coronary artery atherosclerosis revisited in Korean war combat casualties. Arch Pathol Lab Med 1987; 111: 972-976.
[6] Wilson PW, Kauppila LI, O'Donnell CJ, Kiel DP, Hannan M, Polak JM and Cupples LA. Abdominal aortic calcific deposits are an important predictor of vascular morbidity and mortality. Circulation 2001; 103: 1529-1534.
[7] Fiz F, Morbelli S, Piccardo A, Bauckneht M, Ferrarazzo G, Pestarino E, Cabria M, Democrito A, Riondato M, Villavecchia G, Marini C and Sambuceti G. ^{18}F-NaF uptake by atherosclerotic plaque on PET/CT imaging: inverse correlation between calcification density and mineral metabolic activity. J Nucl Med 2015; 56: 1019-1023.
[8] Joshi NV, Vesey AT, Williams MC, Shah AS, Calvert PA, Craighead FH, Yeoh SE, Wallace W, Salter D, Fletcher AM, van Beek EJ, Flapan AD, Uren NG, Behan MW, Cruden NL, Mills NL, Fox KA, Rudd JH, Dweck MR and Newby DE. ^{18}F-fluoride positron emission tomography for identification of ruptured and high-risk coronary atherosclerotic plaques: a prospective clinical trial. Lancet 2014; 383: 705-713.
[9] Morbelli S, Fiz F, Piccardo A, Picori L, Massollo M, Pestarino E, Marini C, Cabria M, Democrito A, Cittadini G, Villavecchia G, Bruzzi P, Alavi A and Sambuceti G. Divergent determinants of ^{18}F-NaF uptake and visible calcium deposition in large arteries: relationship with Framingham risk score. Int J Cardiovasc Imaging 2014; 30: 439-447.
[10] Fiz F, Morbelli S, Bauckneht M, Piccardo A, Ferrarazzo G, Nieri A, Artom N, Cabria M, Marini C, Canepa M and Sambuceti G. Correlation between thoracic aorta ^{18}F-natrium fluoride uptake and cardiovascular risk. World J Radiol 2016; 8: 82-89.
[11] Beheshti M, Saboury B, Mehta NN, Torigian DA, Werner T, Mohler E, Wilensky R, Newberg AB, Basu S, Langsteger W and Alavi A. Detection and global quantification of cardiovascular molecular calcification by fluoro18-fluoride positron emission tomography/computed tomography--a novel concept. Hell J Nucl Med 2011; 14: 114-120.
[12] Hansson GK and Libby P. The immune response in atherosclerosis: a double-edged sword. Nat Rev Immunol 2006; 6: 508-519.
[13] Willerson JT. Systemic and local inflammation in patients with unstable atherosclerotic plaques. Prog Cardiovasc Dis 2002; 44: 469-478.
[14] Shanahan CM. Vascular calcification. Curr Opin Nephrol Hypertens 2005; 14: 361-367.
[15] Doherty TM, Fitzpatrick LA, Inoue D, Qiao JH, Fishbein MC, Detrano RC, Shah PK and Rajavashisth TB. Molecular, endocrine, and genetic mechanisms of arterial calcification. Endocr Rev 2004; 25: 629-672.
[16] Heymann MF, Herisson F, Davaine JM, Charrier C, Battaglia S, Passuti N, Lambert G, Goueffic Y and Heymann D. Role of the OPG/RANK/RANKL triad in calcifications of the atheromatous plaques: comparison between carotid and femoral beds. Cytokine 2012; 58: 300-306.
[17] Davaine JM, Quillard T, Chatelais M, Guilbaud F, Brion R, Guyomarch B, Brennan MA, Heymann D, Heymann MF and Goueffic Y. Bone like arterial calcification in femoral atherosclerotic lesions: prevalence and role of osteoprotegerin and pericytes. Eur J Vasc Endovasc Surg 2016; 51: 259-267.
[18] Cummings SR, San Martin J, McClung MR, Siris ES, Eastell R, Reid IR, Delmas P, Zoog HB, Austin M, Wang A, Kutilek S, Adami S, Zanchetta J, Libanati C, Siddhanti S, Christiansen C and Trial F. Denosumab for prevention of fractures in postmenopausal women with osteoporosis. N Engl J Med 2009; 361: 756-765.
[19] D'Amelio P, Isaia G and Isaia GC. The osteoprotegerin/RANK/RANKL system: a bone key to vascular disease. J Endocrinol Invest 2009; 32: 6-9.
[20] Kiechl S, Werner P, Knoflach M, Furtner M, Willeit J and Schett G. The osteoprotegerin/RANK/RANKL system: a bone key to vascular disease. Expert Rev Cardiovasc Ther 2006; 4: 801-811.
[21] Kiel DP, Kauppila LI, Cupples LA, Hannan MT, O'Donnell CJ and Wilson PW. Bone loss and the progression of abdominal aortic calcification over a 25 year period: the Framingham Heart Study. Calcif Tissue Int 2001; 68: 271-276.
[22] Bagger YZ, Tankó LB, Alexandersen P, Qin G, Christiansen C; Prospective Epidemiological Risk Factors Study Group. Radiographic measure of aorta calcification is a site-specific predictor of bone loss and fracture risk at the hip. J Intern Med 2006; 259: 598-605.
[23] Farhat GN, Newman AB, Sutton-Tyrrell K, Matthews KA, Boudreau R, Schwartz AV, Harris T, Tylavsky F, Visser M, Cauley JA; Health ABCS. The association of bone mineral density measures with incident cardiovascular disease in older adults. Osteoporos Int 2007; 18: 999-1008.
[24] Rosa GM, Bauckneht M, Masoero G, Mach F, Quercioli A, Seitun S, Balbi M, Brunelli C, Paro-

di A, Nencioni A, Vuilleumier N and Montecucco F. The vulnerable coronary plaque: update on imaging technologies. Thromb Haemost 2013; 110: 706-722.

[25] Derlin T, Richter U, Bannas P, Begemann P, Buchert R, Mester J and Klutmann S. Feasibility of 18F-sodium fluoride PET/CT for imaging of atherosclerotic plaque. J Nucl Med 2010; 51: 862-865.

[26] Derlin T, Wisotzki C, Richter U, Apostolova I, Bannas P, Weber C, Mester J and Klutmann S. In vivo imaging of mineral deposition in carotid plaque using 18F-sodium fluoride PET/CT: correlation with atherogenic risk factors. J Nucl Med 2011; 52: 362-368.

[27] Evans NR, Tarkin JM, Chowdhury MM, Warburton EA and Rudd JH. PET imaging of atherosclerotic disease: advancing plaque assessment from anatomy to pathophysiology. Curr Atheroscler Rep 2016; 18: 30.

[28] Dweck MR, Chow MW, Joshi NV, Williams MC, Jones C, Fletcher AM, Richardson H, White A, McKillop G, van Beek EJ, Boon NA, Rudd JH and Newby DE. Coronary arterial 18F-sodium fluoride uptake: a novel marker of plaque biology. J Am Coll Cardiol 2012; 59: 1539-1548.

[29] Fiz F, Marini C, Campi C, Massone AM, Podesta M, Bottoni G, Piva R, Bongioanni F, Bacigalupo A, Piana M, Sambuceti G and Frassoni F. Allogeneic cell transplant expands bone marrow distribution by colonizing previously abandoned areas: an FDG PET/CT analysis. Blood 2015; 125: 4095-4102.

[30] Fiz F, Marini C, Piva R, Miglino M, Massollo M, Bongioanni F, Morbelli S, Bottoni G, Campi C, Bacigalupo A, Bruzzi P, Frassoni F, Piana M and Sambuceti G. Adult advanced chronic lymphocytic leukemia: computational analysis of whole-body CT documents a bone structure alteration. Radiology 2014; 271: 805-813.

[31] Sambuceti G, Brignone M, Marini C, Massollo M, Fiz F, Morbelli S, Buschiazzo A, Campi C, Piva R, Massone AM, Piana M and Frassoni F. Estimating the whole bone-marrow asset in humans by a computational approach to integrated PET/CT imaging. Eur J Nucl Med Mol Imaging 2012; 39: 1326-1338.

[32] Marini C, Bruno S, Fiz F, Campi C, Piva R, Cutrona G, Matis S, Nieri A, Miglino M, Ibatici A, Maria Orengo A, Maria Massone A, Neumaier CE, Totero D, Giannoni P, Bauckneht M, Pennone M, Tenca C, Gugiatti E, Bellini A, Borra A, Tedone E, Efeturk H, Rosa F, Emionite L, Cilli M, Bagnara D, Brucato V, Bruzzi P, Piana M, Fais F and Sambuceti G. Functional activation of osteoclast commitment in chronic lymphocytic leukaemia: a possible role for RANK/RANKL pathway. Sci Rep 2017; 7: 14159.

[33] Fiz F, Sahbai S, Campi C, Weissinger M, Dittmann H, Marini C, Piana M, Sambuceti G and la Fougere C. Tumor burden and intraosseous metabolic activity as predictors of bone marrow failure during radioisotope therapy in metastasized prostate cancer patients. Biomed Res Int 2017; 2017: 3905216.

[34] Chen HY, Chiu YL, Hsu SP, Pai MF, Yang JY and Peng YS. Relationship between Fetuin A, vascular calcification and fracture risk in dialysis patients. PLoS One 2016; 11: e0158789.

[35] Chen Z and Yu Y. Aortic calcification was associated with risk of fractures: a meta-analysis. J Back Musculoskelet Rehabil 2016; 29: 635-642.

[36] Blake GM, Puri T, Siddique M, Frost ML, Moore AEB and Fogelman I. Site specific measurements of bone formation using [(18)F] sodium fluoride PET/CT. Quant Imaging Med Surg 2018; 8: 47-59.

[37] Raynor W, Houshmand S, Gholami S, Emamzadehfard S, Rajapakse CS, Blomberg BA, Werner TJ, Hoilund-Carlsen PF, Baker JF and Alavi A. Evolving role of molecular imaging with ^{18}F-sodium fluoride PET as a biomarker for calcium metabolism. Curr Osteoporos Rep 2016; 14: 115-125.

[38] Czernin J, Satyamurthy N and Schiepers C. Molecular mechanisms of bone ^{18}F-NaF deposition. J Nucl Med 2010; 51: 1826-1829.

[39] Harper E, Rochfort KD, Forde H, Davenport C, Smith D and Cummins PM. TRAIL attenuates RANKL-mediated osteoblastic signalling in vascular cell mono-culture and co-culture models. PLoS One 2017; 12: e0188192.

[40] Bone HG, Chapurlat R, Brandi ML, Brown JP, Czerwinski E, Krieg MA, Mellstrom D, Radominski SC, Reginster JY, Resch H, Ivorra JA, Roux C, Vittinghoff E, Daizadeh NS, Wang A, Bradley MN, Franchimont N, Geller ML, Wagman RB, Cummings SR and Papapoulos S. The effect of three or six years of denosumab exposure in women with postmenopausal osteoporosis: results from the FREEDOM extension. J Clin Endocrinol Metab 2013; 98: 4483-4492.

[41] Weber MH, Burch S, Buckley J, Schmidt MH, Fehlings MG, Vrionis FD and Fisher CG. Instability and impending instability of the thoracolumbar spine in patients with spinal metastases: a systematic review. Int J Oncol 2011; 38: 5-12.

[42] Scheyerer MJ, Pietsch C, Zimmermann SM, Osterhoff G, Simmen HP and Werner CM. SPECT/CT for imaging of the spine and pelvis in clinical routine: a physician's perspective of the adoption of SPECT/CT in a clinical setting with a focus on trauma surgery. Eur J Nucl Med Mol Imaging 2014; 41 Suppl 1: S59-66.